

Nodeless superconductivity of single-crystalline $K_xFe_{2-y}Se_2$ revealed by the low-temperature specific heat

B. Zeng,¹ B. Shen,¹ G. F. Chen,² J. B. He,² D. M. Wang,² C. H. Li,¹ and H. H. Wen^{1,3,*}

¹*Institute of Physics and Beijing National Laboratory for Condensed Matter Physics, Chinese Academy of Sciences, P.O. Box 603, Beijing 100190, China*

²*Department of Physics, Renmin University of China, Beijing 100872, China*

³*National Laboratory of Solid State Microstructures and Department of Physics, Nanjing University, Nanjing 210093, China*

(Received 26 January 2011; revised manuscript received 10 March 2011; published 18 April 2011)

Low-temperature specific heat (SH) has been measured in $K_xFe_{2-y}Se_2$ single crystals with $T_c = 32$ K. The SH anomaly associated with the superconducting transition is moderate and sharp, yielding a value of $\Delta C/T|_{T_c} = 11.6 \pm 1.0$ mJ/mol K². The residual SH coefficient $\gamma(0)$ in the superconducting state at $T \rightarrow 0$ is very small with a value of about 0.39 mJ/mol K². The magnetic-field-induced enhancement of the low-T SH exhibits a rough linear feature indicating a nodeless gap. This is further supported by the scaling based on the nodeless-gap approach of the low-T data at different magnetic fields. A rough estimate indicates that the normal-state SH coefficient γ_n is about 6 ± 0.5 mJ/mol K², leading to $\Delta C/\gamma_n T|_{T_c} = 1.93$ and placing this superconductor in the strong coupling region.

DOI: [10.1103/PhysRevB.83.144511](https://doi.org/10.1103/PhysRevB.83.144511)

PACS number(s): 74.70.Xa, 74.20.Rp, 74.62.Dh, 65.40.Ba

I. INTRODUCTION

The discovery of high-temperature superconductivity in iron pnictides has opened an era in the investigation of this superconducting mechanism.¹ One of the key issues here is about the superconducting pairing mechanism. Experimentally, it was found that the superconductivity is at the vicinity of a long-range antiferromagnetic (AF) order;² the superconducting transition temperature gets higher when this AF order is suppressed. It was also further proven that the AF spin fluctuation³ and the multiband effect⁴ are two key factors for driving the system into superconductivity. Theoretically, several different pairing symmetries are anticipated. It was suggested that the pairing may be established via inter-pocket scattering of electrons between the hole pockets (around the Γ point) and electron pockets (around the M point), leading to the pairing manner of an isotropic gap on each pocket but with opposite signs between them (the so-called S^\pm).^{5–8} The pairing picture based on the superexchange of local moments was also proposed, which in principle could also lead to S^\pm ,^{9,10} leaving the others (d -wave or full-gapped S^{++}) as perspectives with low possibility. However, the S^{++} pairing manner is, in particular, winning the vote when the orbital fluctuation plays the important role, as argued by Onari and Kontani.¹¹ Clearly multiorbits, or the naturally formed multipockets are highly desirable for the superconductivity of all these pairing models.

Recently, an Fe-based superconducting system $A_xFe_{2-y}Se_2$ (A = alkaline metals, $x \leq 1$, $y \leq 0.5$) was discovered with a transition temperature above 30 K.¹² The interest in this fascinating system was immediate because of the two major reasons: (1) Both the band-structure calculations^{13,14} and the preliminary angle resolved photoemission spectrum (ARPES) measurements^{15–17} indicate that the band near the Γ point seems to dive far below the Fermi energy, leading to the absence of hole pockets which are widely expected for the FeAs-based systems. A consequence of these results is to question the importance of the inter-hole-electron-pocket scattering for the superconducting pairing. (2) The super-

conducting state seems to occur via a transmutation from an insulating ordered state of Fe vacancies.¹⁸ The question raised here is whether this insulating state originates from the Mottness, like in the cuprate,¹⁹ or from the band gap due to the reconstruction of the electronic structure when the Fe vacancies are present. Many different kinds of pairing symmetries are proposed, such as nodeless d -wave,²⁰ S^{++} , or S^\pm , and all are satisfying with the basic structures. To date, experimental evidence about the superconducting gaps is quite rare. The ARPES measurements indicate isotropic gaps on the four-electron pockets with a rather large gap value (~ 8 – 15 meV). The conclusions drawn from nuclear magnetic resonance (NMR) measurements seem controversial.^{21,22} In this paper, we present data of low-temperature specific-heat (SH) measurements. Our detailed analysis indicates a nodeless gap with a strong coupling strength in this superconducting system.

II. SAMPLE PREPARATION AND EXPERIMENTAL TECHNIQUES

The $K_xFe_{2-y}Se_2$ single crystals were synthesized by the flux-growth method.²³ The typical dimension of the samples for specific-heat measurements was $2 \times 2 \times 0.5$ mm³. The SH measurements were done with the thermal relaxation method on a Quantum Design instrument physical property measurement system (PPMS) with the temperature down to 2 K and magnetic field up to 9 T. The magnetic field effect on the bare SH measuring chip (including the four thermal conducting wires) of PPMS from Quantum Design was calibrated prior to the measurements on the samples in order to remove the pseudomorphism. This becomes very essential since the contribution of the electronic SH is quite small compared to the phonon part in this particular system. The details about the correction will be presented later in combination with the discussion of experimental data and shown in Figs. 4 and 5. In all the measurements, the magnetic field was applied

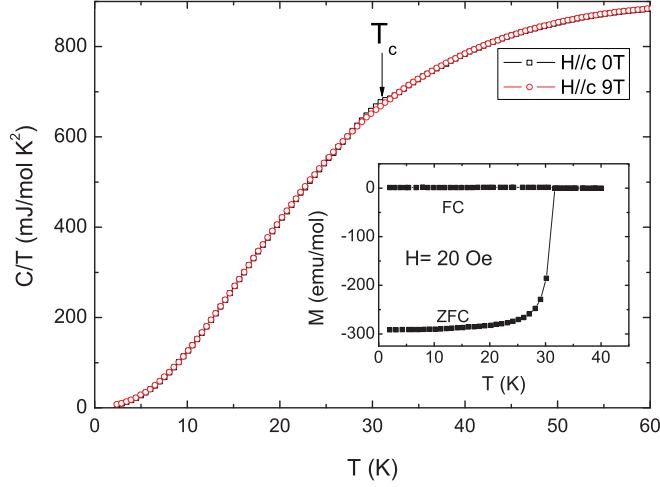


FIG. 1. (Color online) Raw data of the temperature dependence of specific heat for the $K_x\text{Fe}_{2-y}\text{Se}_2$ at 0 and 9 T. The inset shows the temperature dependence of the dc magnetization for the same sample measured under a magnetic field of 20 Oe.

perpendicular to the FeSe planes. The dc magnetization measurements were done with a superconducting quantum interference device (SQUID) from Quantum Design.

III. RESULTS AND DISCUSSION

In Fig. 1, we show the temperature dependence of specific heat and dc magnetization for the sample. The sharp transition in the magnetization and the large magnetic screening signal indicate the good quality of the sample. In the SH data at zero field, one can see a small feature of heat capacity anomaly at T_c . We will show that this SH anomaly is actually rather sharp with a reasonable magnitude.

The SH data for the sample in the low-temperature region are plotted as C/T vs. T^2 in the inset of Fig. 2. No Schottky anomaly was detected. The data below about 8 K can be fit by

$$C(T, H) = \gamma(H)T + \beta T^3 + \eta T^5, \quad (1)$$

where $\gamma(H)T$ is the residual SH coefficient in the magnetic field H and $\beta T^3 + \eta T^5$ is the phonon part of heat capacity. Normally it is unnecessary to consider the last term ηT^5 in the low-temperature region, but this seems not to be the case for the present sample. One can see a slight upturn curvature in the low-T SH data C/T vs. T^2 . This is understood because of the relatively low Debye temperature of the sample, as discussed below.

For the heat capacity of the sample, the phonon contribution should be identical in zero and nonzero magnetic field. Hence, the parameters β and η should be the same for 0 and 9 T. This is a constraint in the fitting process of the data. By fitting the SH data at 0 and 9 T using Eq. (1), we obtained $\gamma(0) \approx 0.394$ mJ/mol K², $\gamma(9 \text{ T}) \approx 1.4$ mJ/mol K², $\beta \approx 1.018$ mJ/mol K⁴, and $\eta \approx 0.003$ mJ/mol K⁶. Using the obtained value of β and the relation $\Theta_D = [12\pi^4 k_B N_A Z / (5\beta)]^{1/3}$, where $N_A = 6.02 \times 10^{23} \text{ mol}^{-1}$ is the Avogadro constant and $Z = 5$ is the number of atoms in one unit cell, we get the Debye temperature $\Theta_D \approx 212$ K, which is relatively small compared to other FeAs-based superconductors.^{24,25}

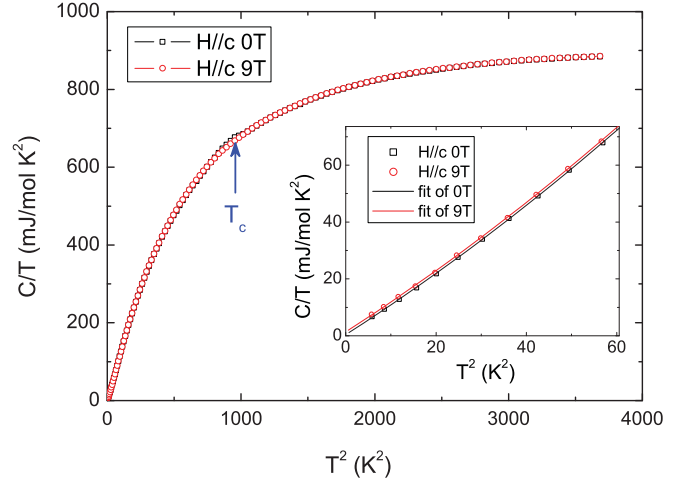


FIG. 2. (Color online) Main panel shows the SH data plotted as C/T vs. T^2 . The inset shows an enlarged view of the data together with the fit (see text) in the low-temperature region. No Schottky anomaly was detected.

Figure 3(a) shows an enlarged view of the SH data near the transition temperature plotted as C/T vs. T . One can see a clear SH anomaly at T_c at 0 T and, when a magnetic field is applied, the SH anomaly was weakened and shifted to lower temperatures. Figure 3(b) shows the difference of the SH data between 0 and 9 T. The SH anomaly at T_c is more obvious. We can evaluate the height of the SH anomaly

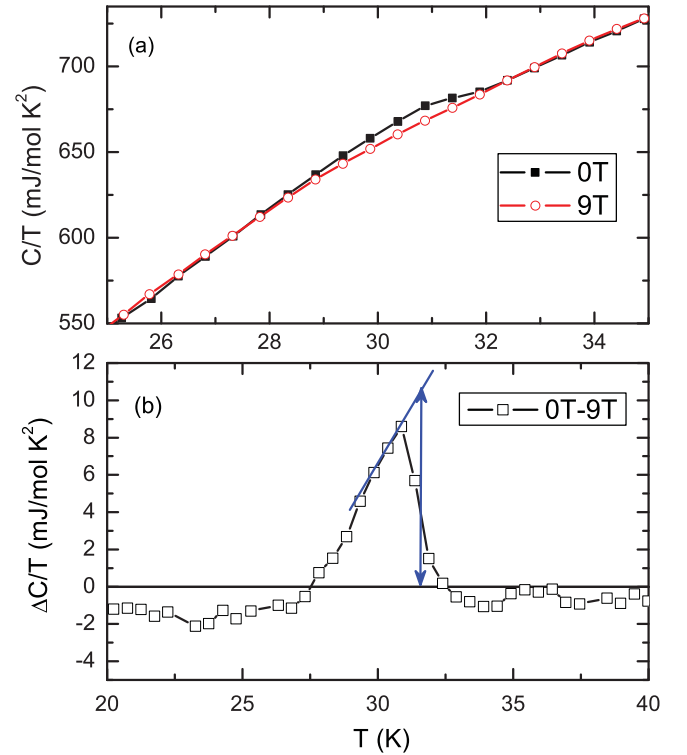


FIG. 3. (Color online) Upper panel shows an enlarged view of the SH data near the transition temperature plotted as C/T vs. T . The lower panel shows the difference in the SH data between 0 and 9 T. The blue solid lines here are just guides to the eye to show how we determine the height of the SH anomaly.

$\Delta C/T|_{T_c}$ near T_c from the difference of C/T at 0 and 9 T. The estimated anomaly $\Delta C/T|_{T_c}$ is about 11.6 ± 1 mJ/mol K². For the optimally doped (Ba,K)Fe₂As₂ and Ba(Fe,Co)₂As₂, the SH anomaly $\Delta C/T|_{T_c}$ is about 98 and 28.6 mJ/mol K², respectively.^{25–29} The SH anomaly for K_xFe_{2–y}Se₂ is also smaller than other FeAs-based superconductors. It is also found that the empirical relation $\Delta C/T|_{T_c} \propto T_c^2$ observed in K-doped or Co (Ni)-doped FeAs-122²⁶ does not apply here. This may be induced by the possible missing of the hole pocket, which leads to smaller $\Delta C/T_c$ in A_xFe_{2–y}Se₂. The SH anomaly looks rather sharp (it starts at about 32.9 K and ends at 30.9 K). We must emphasize that using the data measured at 9 T as the background to deduce the SH anomaly is reasonable. As we discuss below, a magnetic field of 9 T should have lowered the transition temperature by about 5–6 K (with the upper critical field $H_{c2}^*(0) \approx 48$ T), being much larger than the width of the SH anomaly. The rather sharp SH anomaly is very different from that in the underdoped cuprates in which a long tail of electronic SH was observed far into the normal state.³⁰ This was interpreted as fluctuating superconductivity. This may suggest that, although having a low superfluid density and relatively higher anisotropy,³¹ the superconducting transition in A_xFe_{2–y}Se₂ superconductors can still be described quite well by the critical mean-field theory without the necessity of categorizing it into the strong critical fluctuation.

Before proceeding with further analysis of the SH data, we shall illustrate the process of SH measurement and data processing. As mentioned above, the SH measurement was carried out on a Quantum Design PPMS, using the heat capacity (HC) option. In this instrument, the sample is put on a small chip on the back of which are attached two resistors that function as a thermometer and a heater. The sample SH is obtained by subtracting the total SH of the chip and sample from the SH of a bare chip. We use this procedure in different magnetic fields to figure out the behavior of the sample in magnetic fields. But the magnetic fields have little influence on the resistance of the thermometer on the chip (the field dependence of the SH of the chip can be ignored, see the HC manual of PPMS). Theoretically, if we calibrate the resistance of the thermometer in a magnetic field, we could get an accurate value of SH. But in practice, according to our experience, this method cannot fully remove the influence of the magnetic field (we have measured several samples, such as Nb and Au, to test this method). Thus, we take another approach. We do not take the calibration, but measure the SH of the bare chip in the magnetic field directly. As revealed in the data, the SH of the chip, which was supposed to be field-independent, seems field-dependent. This field dependence of the SH of the chip is actually given by the field dependence of the thermometer, and this could be treated as the magnetic field background, as shown in Fig. 4(a). This is a background with systematics and is enlarged proportionally when the sample is mounted on the chip. Therefore, we get the final SH of the sample as $C(H) = C_{\text{meas}}^H - C_{\text{bkg}}(C_{\text{total}}^0/C_{\text{chip}}^0)$, where C_{meas}^H is the measured SH of the sample at a field H , C_{bkg} is the background shown in Fig. 4(a), C_{total}^0 is the total SH of the sample and the chip at zero field, and C_{chip}^0 is the SH data of the chip measured at zero field. By removing this background, we obtain the SH of the sample in a magnetic

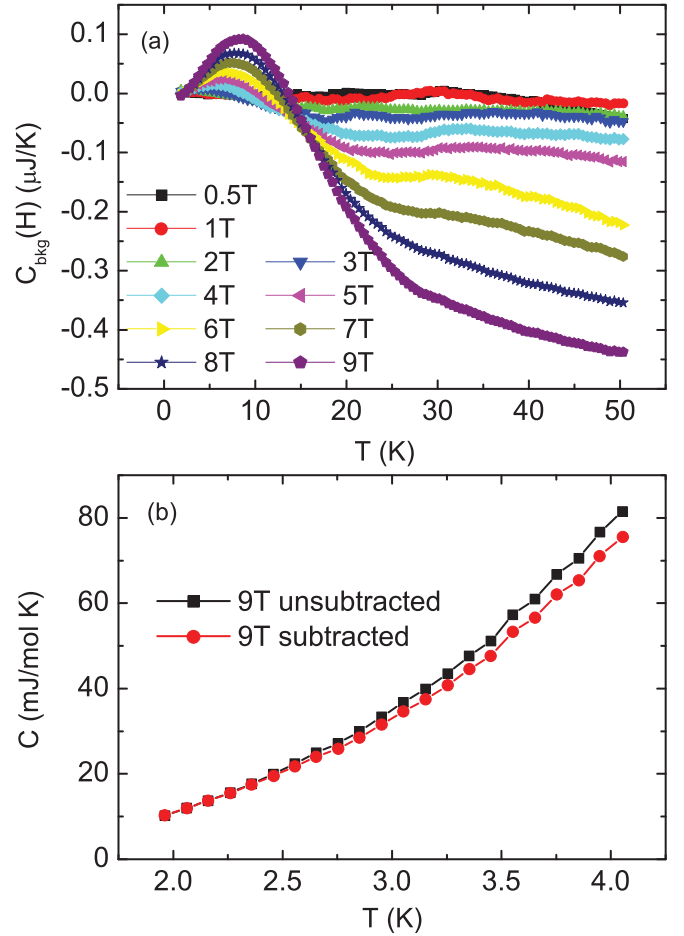


FIG. 4. (Color online) (a) Magnetic field background measured for the bare chip, $C_{\text{bkg}}(H) = C(H) - C(0)$, raw data are plotted as C vs. T . (b) Enlarged view of the SH data of the sample in the low- T region for 9 T, before and after subtracting the background.

field. In our experience, this method works better, and it is also tested by measuring Nb and Au. Here we notice that, although the background is larger in higher temperature, as shown in Fig. 4(a), it actually has little influence on the high- T region of SH data, because the heat capacity increases more rapidly. Even if we only consider the phonon SH, it is a T^3 law with increasing temperature. Usually, the magnetic effect can be ignored above 20 K. In Fig. 4(b), we show the 9-T SH data of the sample in the low- T region before and after subtracting the background. One can see that there is a small correction to the raw data. Although this method works better, there would be still little residual background, which has a larger effect when the electronic SH is small and in high magnetic field, as shown below.

Figure 5 shows the SH data plotted as C/T vs. T^2 in the low-temperature region under various magnetic fields. One can see that the magnetic field enhances the SH coefficient progressively, indicating the generation of the quasiparticle density of states. Panel (a) of Fig. 5 presents the difference in the SH data between a typical magnetic field and zero field and the dashed lines are the linear fit of the difference in the temperature region of 2.4 to 4 K. The slight bending down of the data here below about 2.4 K at fields of 5, 7, and

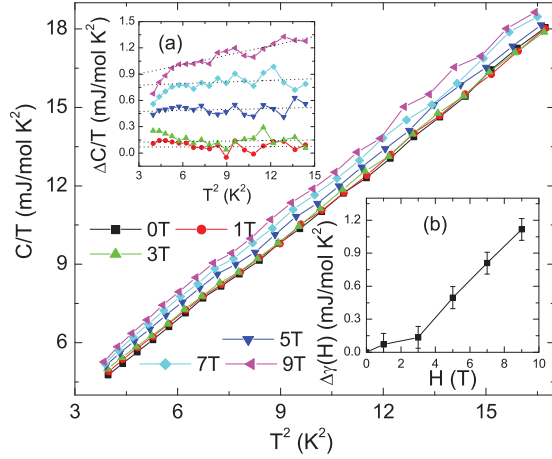


FIG. 5. (Color online) SH data in the low-temperature region under various magnetic fields. Inset (a): The difference in the SH data between a particular magnetic field and zero field. The dashed lines are the linear fit of this difference between 2.4 and 4 K. The slight bending down of the data at 5, 7, and 9 T was recognized as due to the unsuccessful removal of the magnetic field effect on the SH measuring chip. Inset (b): Field dependence of the field-induced term $\Delta\gamma(H) = [C(T, H) - C(T, 0)]/T$ at $T = 3$ K.

9 T was recognized as due to the unsuccessful removal of the magnetic field effect on the SH measuring chip. This would have a more obvious effect on high-magnetic-field data, and especially in the low-T region. As shown in panel (a) of Fig. 5, the difference in SH data for 9 and 0 T is a little tilted, rather than a rough constant, so we extracted the data at $T = 3$ K as the field-induced term of SH. Using the linear fit (between 2.4 and 4 K) in panel (a), we can obtain the magnetic-field-induced enhancement of the low-T SH, and the extracted data at $T = 3$ K are shown in Fig. 5(b). It is clear that the field-induced term exhibits a roughly linear field dependence. This is very different from the cuprates, in which a square-root relation $\Delta\gamma \propto \sqrt{H}$ was observed widely in many kinds of materials.^{32–37} In combination with the fact that a very small residual SH term was observed in the superconducting state of $\text{K}_x\text{Fe}_{2-y}\text{Se}_2$ as $T \rightarrow 0$, we are tempted to conclude a nodeless gap.

In order to further confirm this point, we analyzed the SH data in the finite-temperature region in the mixed state. It is known that the quasiparticle excitations in superconductors with different gap symmetries can be obviously distinct. In s -wave superconductors, the inner-core states dominate the quasiparticle excitations and, consequently, a simple scaling law $C_{\text{QP}}/T^3 \approx C_{\text{core}}/T^3 = \gamma_n/H_{c2}(0) \times (T/\sqrt{H})^{-2}$ for the fully gapped superconductors is expected, where C_{QP} and C_{core} are the specific heat of the quasiparticles induced by field and that from the vortex cores in the mixed state, respectively. This scaling was proposed by Liu *et al.*³⁸ for the possible s -wave gap in electron-doped cuprate superconductor $\text{Sr}_{0.9}\text{La}_{0.1}\text{CuO}_4$. Here we use the T/\sqrt{H} as the variable in order to have a comparison with the d -wave. Although for the nodeless d -wave and S^{++} we do not have the available theoretical formula, for the low-energy density of states (DOS) under a field we would assume that they behave more like the case of a full gap; here, we generally call it

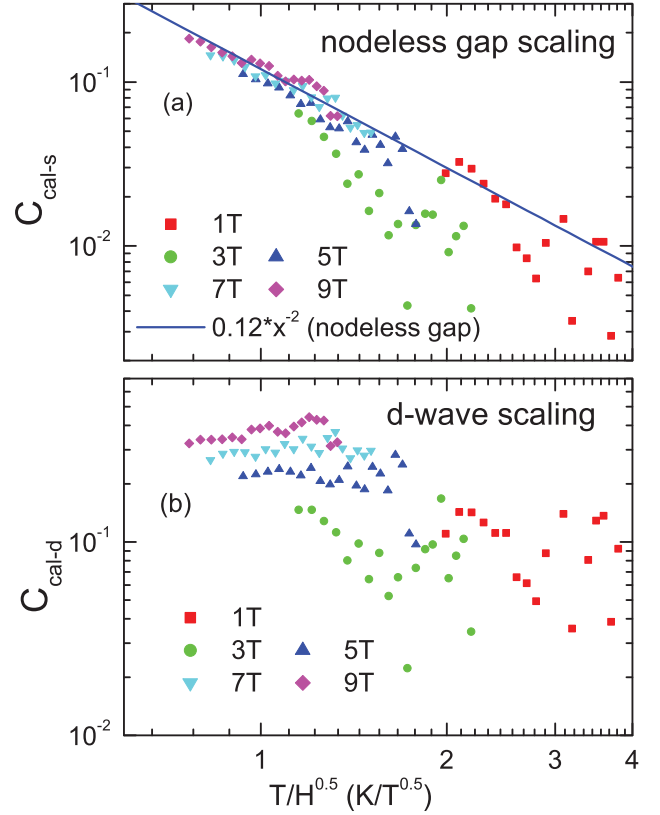


FIG. 6. (Color online) (a) Scaling of the data according to the nodeless-gap scenario (symbols) $C_{\text{cal-s}} = [C(H) - C(0)]/T^3$ vs. T/\sqrt{H} , the dashed line represents the theoretical expression. (b) Scaling of the data (symbols) based on d -wave prediction $C_{\text{cal-d}} = [C(H) - C(0)]/T\sqrt{H}$ vs. T/\sqrt{H} . No good scaling can be found for the d -wave case.

a nodeless gap. Therefore, we will adopt this scaling of a nodeless gap to check our present sample. For a gap with line nodes, the excitation spectrum is dominated by the extended quasiparticles outside the vortex cores and the so-called Simon-Lee scaling law³⁹ $C_{\text{QP}}/(T/\sqrt{H}) \approx C_{\text{Vol}}/(T/\sqrt{H}) = f(T/\sqrt{H})$ should be obeyed, where C_{Vol} is the specific heat of the extended states outside the vortex cores predicted by Volovik.⁴⁰ The scaling result of the field-induced term in the mixed state with the nodeless condition is presented in Fig. 6(a) and the d -wave scaling is shown in Fig. 6(b). One can see that the nodeless scaling is better than the d -wave scaling; all the data at different magnetic fields can be roughly scaled to the straight blue line in Fig. 6(a), which reflects the theoretical curve $C_{\text{cal-s}} = 0.12(T/\sqrt{H})^{-2}$. Generally, this prefactor $\gamma_n/H_{c2}(0) = 0.12$ mJ/(mol K² T) is consistent with the magnitude of the slope of the line in Fig. 5(b). Using the value of $H_{c2}^c(0) \approx 48$ T,²³ we estimate the value of normal-state electron SH coefficient γ_n to be 5.8 mJ/mol K², which is a small value compared to other FeAs-based superconductors.^{25–29}

As far as we know, reliable calculated values for the normal-state DOS and thus the SH coefficient of this superconductor are still lacking because of the uncertainties in the structure of these Fe vacancies. The value $\gamma_n \approx 6$ mJ/mol K² found here will give some hint about the band-structure calculations

as well as help in understanding the ARPES data. The value $\Delta C/\gamma_n T|_{T_c} = 1.93$ clearly places the system in the strong coupling camp, since the weak coupling BCS theory gives 1.43. Furthermore, the very small residual SH coefficient $\gamma(0) \approx 0.39$ mJ/mol K² together with the nodeless-gap scaling excludes nodal gaps in this system. This is consistent with the ARPES data to date and in contradiction with the NMR data.²² The small $\gamma(0)$ detected here excludes also the chemical phase separation picture, since otherwise a much more significant value, arising from the nonsuperconducting normal metallic regions, should be observed. However, if the system is chemically separated into the superconducting regions and the insulating regions which are fully gapped (for example, the Fe vacancies are ordered), this is of course acceptable. Our results here are also probably against the nodeless-*d*-wave picture since that kind of pairing may be sensitive to impurity scattering, as for S^\pm pairing,⁴¹ which would give rise to a large quasiparticle DOS provided the appropriate scattering potentials are present, and this large DOS should be detectable by specific heat. The sharp SH anomaly found here indicates that the present system does not have the strong critical fluctuation which appears in the underdoped cuprates.

IV. SUMMARY

In summary, we measured the low-temperature SH of single-crystal $K_x\text{Fe}_{2-y}\text{Se}_2$ in various magnetic fields. The SH anomaly is observed at $T_c = 32$ K and the height $\Delta C/T|_{T_c}$ is about 11.6 mJ/mol K². From the low-temperature part of the SH data, we obtained the field-induced enhancement of the low-T SH, which exhibits a roughly linear field dependence, indicating a nodeless gap. We also analyzed the data with the *s*-wave scaling law, and found that the data roughly obey this law, indicating again a nodeless gap. These approaches are self-consistent with each other. The Debye temperature and the normal-state electronic SH coefficient were also estimated; both are smaller than that found in other FeAs-based superconductors.

ACKNOWLEDGMENTS

We appreciate the useful discussions with Hong Ding, Doug Scalapino, and Tao Xiang. This work is supported by the NSF of China, the Ministry of Science and Technology of China (973 projects: 2011CBA001000), and Chinese Academy of Sciences.

*hhwen@nju.edu.cn

¹Y. Kamihara, T. Watanabe, M. Hirano, and H. Hosono, *J. Am. Chem. Soc.* **130**, 3296 (2008).

²C. de la Cruz, Q. Huang, J. W. Lynn, J. Li, W. Ratcliff II, J. L. Zarestky, H. A. Mook, G. F. Chen, J. L. Luo, N. L. Wang, and P. C. Dai, *Nature (London)* **453**, 899 (2008).

³F. L. Ning, K. Ahilan, T. Imai, A. S. Sefat, M. A. McGuire, B. C. Sales, D. Mandrus, P. Cheng, B. Shen, and H. H. Wen, *Phys. Rev. Lett.* **104**, 037001 (2010).

⁴L. Fang, H. Q. Luo, P. Cheng, Z. S. Wang, Y. Jia, G. Mu, B. Shen, I. I. Mazin, L. Shan, C. Ren, and H. H. Wen, *Phys. Rev. B* **80**, 140508 (2009).

⁵I. I. Mazin, D. J. Singh, M. D. Johannes, and M. H. Du, *Phys. Rev. Lett.* **101**, 057003 (2008).

⁶K. Kuroki, S. Onari, R. Arita, H. Usui, Y. Tanaka, H. Kontani, and H. Aoki, *Phys. Rev. Lett.* **101**, 087004 (2008).

⁷F. Wang, H. Zhai, Y. Ran, A. Vishwanath, and D. H. Lee, *Phys. Rev. Lett.* **102**, 047005 (2009).

⁸Z. J. Yao, J. X. Li, and Z. D. Wang, *New J. Phys.* **11**, 025009 (2009).

⁹K. Seo, B. A. Bernevig, and J. Hu, *Phys. Rev. Lett.* **101**, 206404 (2008).

¹⁰Q. Si and E. Abrahams, *Phys. Rev. Lett.* **101**, 076401 (2008).

¹¹S. Onari and H. Kontani, *Phys. Rev. Lett.* **103**, 177001 (2009).

¹²J. Guo, S. Jin, G. Wang, S. Wang, K. Zhu, T. Zhou, M. He, and X. L. Chen, *Phys. Rev. B* **82**, 180520 (2010).

¹³I. A. Nebrasov and M. V. Sadovskii, e-print [arXiv:1101.0051](https://arxiv.org/abs/1101.0051) (2011).

¹⁴X. W. Yan, M. Gao, Z. Y. Lu, and T. Xiang, e-print [arXiv:1012.5536](https://arxiv.org/abs/1012.5536) (2011).

¹⁵Y. Zhang, L. X. Yang, M. Xu, Z. R. Ye, F. Chen, C. He, J. Jiang, B. P. Xie, J. J. Ying, X. F. Wang, X. H. Chen, J. P. Hu, D. L. Feng, e-print [arXiv:1012.5980](https://arxiv.org/abs/1012.5980).

¹⁶T. Qian, X. P. Wang, W. C. Jin, P. Zhang, P. Richard, G. Xu, X. Dai, Z. Fang, J. G. Guo, X. L. Chen, and H. Ding, e-print [arXiv:1012.6017](https://arxiv.org/abs/1012.6017).

¹⁷D. X. Mou, S. Y. Liu, X. W. Jia, J. F. He, Y. Y. Peng, L. Zhao, L. Yu, G. D. Liu, S. L. He, X. L. Dong, J. Zhang, H. D. Wang, C. Dong, M. H. Fang, X. Wang, Q. Peng, Z. Wang, S. J. Zhang, F. Yang, Z. Y. Xu, C. T. Chen, and X. J. Zhou, e-print [arXiv:1101.4556](https://arxiv.org/abs/1101.4556).

¹⁸M. H. Fang, H. D. Wang, C. Dong, Z. Li, C. Feng, J. Chen, and H. Q. Yuan, e-print [arXiv:1012.5236](https://arxiv.org/abs/1012.5236).

¹⁹Rong Yu, Jian-Xin Zhu, and Qimiao Si, e-print [arXiv:1101.3307](https://arxiv.org/abs/1101.3307).

²⁰F. Wang, F. Yang, M. Gao, Z. Y. Lu, T. Xiang, and D. H. Lee, e-print [arXiv:1101.4390](https://arxiv.org/abs/1101.4390).

²¹W. Q. Yu, L. Ma, J. B. He, D. M. Wang, T. L. Xia, and G. F. Chen, e-print [arXiv:1101.1017](https://arxiv.org/abs/1101.1017).

²²H. Kotegawa, Y. Hara, H. Nohara, H. Tou, Y. Mizuguchi, H. Takeya, and Y. Takano, e-print [arXiv:1101.4572](https://arxiv.org/abs/1101.4572).

²³D. M. Wang, J. B. He, T.-L. Xia, and G. F. Chen, e-print [arXiv:1101.0789](https://arxiv.org/abs/1101.0789).

²⁴G. Mu, X. Y. Zhu, L. Fang, L. Shan, C. Ren, and H. H. Wen, *Chin. Phys. Lett.* **25**, 2221 (2008).

²⁵G. Mu, H. Q. Luo, Z. S. Wang, L. Shan, C. Ren, and H. H. Wen, *Phys. Rev. B* **79**, 174501 (2009).

²⁶S. L. Bud'ko, Ni Ni, and P. C. Canfield, *Phys. Rev. B* **79**, 220516 (2009).

²⁷K. Gofryk, A. S. Sefat, M. A. McGuire, B. C. Sales, D. Mandrus, J. D. Thompson, E. D. Bauer, and F. Ronning, *Phys. Rev. B* **81**, 184518 (2010).

²⁸P. Popovich, A. V. Boris, O. V. Dolgov, A. A. Golubov, D. L. Sun, C. T. Lin, R. K. Kremer, and B. Keimer, *Phys. Rev. Lett.* **105**, 027003 (2010).

²⁹G. Mu, B. Zeng, P. Cheng, Z. S. Wang, L. Fang, B. Shen, L. Shan, C. Ren, and H. H. Wen, *Chin. Phys. Lett.* **27**, 037402 (2010).

- ³⁰H. H. Wen, G. Mu, H. Q. Luo, H. Yang, L. Shan, C. Ren, P. Cheng, J. Yan, and L. Fang, *Phys. Rev. Lett.* **103**, 067002 (2009).
- ³¹C. H. Li, B. Shen, F. Han, X. Y. Zhu, and H. H. Wen, e-print [arXiv:1012.5637](https://arxiv.org/abs/1012.5637).
- ³²K. A. Moler, D. J. Baar, J. S. Urbach, Ruixing Liang, W. N. Hardy, and A. Kapitulnik, *Phys. Rev. Lett.* **73**, 2744 (1994); K. A. Moler, John R. Kirtley, Ruixing Liang, Douglas Bonn, and Walter N. Hardy, *Phys. Rev. B* **55**, 12753 (1997).
- ³³B. Revaz, J.-Y. Genoud, A. Junod, K. Neumaier, A. Erb, and E. Walker, *Phys. Rev. Lett.* **80**, 3364 (1998).
- ³⁴D. A. Wright, J. P. Emerson, B. F. Woodfield, J. E. Gordon, R. A. Fisher, and N. E. Phillips, *Phys. Rev. Lett.* **82**, 1550 (1999).
- ³⁵R. A. Fisher, B. Buffeteau, R. Calemczuk, K. W. Dennis, T. E. Hargreaves, C. Marcenat, R. W. McCallum, A. S. O'Connor, N. E. Phillips, and A. Schilling, *Phys. Rev. B* **61**, 1473 (2000).
- ³⁶N. E. Phillips, R. A. Fisher, A. Schilling, B. Buffeteau, T. E. Hargreaves, C. Marcenat, R. Calemczuk, A. S. O'Connor, K. W. Dennis, and R. W. McCallum, *Physica B* **259-261**, 546 (1999).
- ³⁷H. H. Wen, Z. Y. Liu, F. Zhou, J. W. Xiong, W. X. Ti, T. Xiang, S. Komiya, X. F. Sun, and Y. Ando, *Phys. Rev. B* **70**, 214505 (2004); H. H. Wen, L. Shan, X. G. Wen, Y. Wang, H. Gao, Z. Y. Liu, F. Zhou, J. W. Xiong, and W. X. Ti, *ibid.* **72**, 134507 (2005).
- ³⁸Z. Y. Liu, H. H. Wen, L. Shan, H. P. Yang, X. F. Lu, H. Gao, Min-Seok Park, C. U. Jung, and Sung-Ik Lee, *Europhys. Lett.* **69**, 263 (2005).
- ³⁹S. H. Simon and P. A. Lee, *Phys. Rev. Lett.* **78**, 1548 (1997).
- ⁴⁰G. E. Volovik, *JETP Lett.* **58**, 469 (1993); **65**, 491 (1997).
- ⁴¹T. Kariyado and M. Ogata, *J. Phys. Soc. Jpn.* **79**, 083704 (2010).